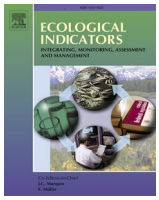
Ecological Indicators 171 (2025) 113181



Contents lists available at ScienceDirect

Ecological Indicators

journal homepage: www.elsevier.com/locate/ecolind



Original Articles

Temporal analyses of global suitability distribution for fall armyworm based on Multiple factors

Minghao Wang [a,b], Wenjiang Huang [a,b,*], Yingying Dong [a,b,*], Yanru Huang [a,b], Bing Zhang [a,b], Gang Sun [a,b], Maged Elkahky [c], Changping Huang [b,d]

[a] Key Laboratory of Remote Sensing and Digital Earth, Aerospace Information Research Institute, Chinese Academy of Sciences, Beijing 100101, China
[b] University of Chinese Academy of Sciences, Beijing 100049, China
[c] Food and Agriculture Organization of the United Nations, FAO, Roma, Italy
[d] National Engineering Laboratory for Satellite Remote Sensing Applications, Aerospace Information Research Institute, Chinese Academy of Sciences, Beijing 100094, China

ARTICLE INFO

Keywords:
Spodoptera frugiperda
MaxEnt
Potential distribution
Static and dynamic environmental factors

ABSTRACT

The fall armyworm (FAW; Spodoptera frugiperda) has been a persistent threat to global food security due to its strong migratory ability and wide range of host plants. However, most current studies on the suitability distribution of FAW focus on extracting suitable areas in specific regions on an annual basis. Consequently, research on the suitability distribution of FAW at a larger scale and with higher temporal resolution is urgently needed to provide data support for early prevention and control. This study differentiated the historical occurrence records of FAW into annual distribution points and seasonal distribution points. By integrating multi-factor environmental data, including climate, soil, topography, and vegetation, we used MaxEnt to establish annual and monthly models. The annual model extracted the annual suitability distribution of FAW worldwide. Among the nine selected environmental factors, temperature seasonality had the greatest impact on the suitability distribution of FAW, with a single-factor contribution rate of 39.87%. The monthly models analyzed the inter-monthly variations in the global suitability distribution of FAW from January to December. The results indicated that FAW's suitability was highest in July and lowest in March. Under the dominant influence of dynamic environmental factors such as temperature, precipitation, and vegetation index, the expansion and contraction of FAW's suitability distribution corresponded with seasonal changes, exhibiting significant seasonal fluctuations. Our results can provide FAW control personnel with more practical references for formulating preventive strategies in advance, helping to prevent the potentially incalculable damage FAW could cause to crops in invaded areas.

1. Introduction

The fall armyworm (FAW; *Spodoptera frugiperda*) (Lepidoptera: Noctuidae) originates from tropical and subtropical regions of the Americas (Sparks, 1979) and is a significant agricultural pest with strong polyphagy and migratory behavior. FAW larvae can feed on at least 353 host plants from 76 plant families (Montezano et al., 2018), including more than 100 important economic crops such as maize, sorghum from the Poaceae family, and soybean from the Fabaceae family (De Freitas Bueno, 2011; Hardke et al., 2015; Pitre and Hogg, 1983). The polyphagous nature of FAW indicates a potential risk to economic crops worldwide. Additionally, due to the lack of a diapause mechanism, the annual suitability distribution of FAW is limited to relatively warm and humid regions (Early et al., 2018). However, the adults possess strong migratory capabilities, enabling them to travel hundreds of kilometers in a single night with the assistance of wind currents (Westbrook et al., 2016). In the Americas, FAW lives throughout the year, extending its range from La Pampa in Argentina to southern Florida and Texas in the USA. During the growing season, it migrates seasonally, extending its range northward to regions such as Québec and Ontario in Canada (Early et al., 2018). The rapid spread of FAW within continents is facilitated by its migratory ability; however, its long-distance intercontinental dissemination is primarily achieved through air and maritime transportation. Between 2016 and 2018, FAW caused severe pest outbreaks in 44 African countries (Matova et al., 2020; Otim et al., 2018; Sisay et al., 2019). In 2018, FAW was first detected in India, marking its

* Corresponding authors.
E-mail addresses: huangwj@aircas.ac.cn (W. Huang), dongyy@aircas.ac.cn (Y. Dong).

https://doi.org/10.1016/j.ecolind.2025.113181
Received 15 September 2024; Received in revised form 13 January 2025; Accepted 30 January 2025
Available online 3 February 2025
1470-160X/© 2025 The Authors. Published by Elsevier Ltd. This is an open access article under the CC BY license (http://creativecommons.org/licenses/by/4.0/).

initial invasion into Asia and its rapid spread northward and northeastward across the region (Suby et al., 2020). Subsequently, neighboring countries such as Bangladesh, Myanmar, Sri Lanka, Nepal, and China also experienced infestations (Suby et al., 2020). Given the continuous increase in global trade and ongoing climate change, it is anticipated that the impact of FAW infestations will become more severe (Kenis et al., 2023). Therefore, understanding the suitability distribution for FAW on a global scale and deploying early prevention and control measures are particularly crucial.

Species distribution models (SDMs) are presently a highly efficient approach for forecasting the potential distribution of invasive species (Kumar et al., 2014). Environmental variables are the core inputs of SDMs, providing descriptions and predictions of the ecological conditions affecting species distribution. Early et al. (2018) integrated native and African distribution data with meteorological data on FAW life-history to construct SDMs. Liu et al. (2020) explored the impacts of land-use change, topography, and climate change on the distribution pattern of FAW. Most of these studies only use natural geographical conditions as input for the environmental data layer. However, the status of surface vegetation cover within a region also has a significant impact on the occurrence process of FAW populations (Fan et al., 2021). Remote sensing data, due to its advantages of large-scale spatial observation, long-term dynamic monitoring, fast speed, and low cost (Giri, 2016), can represent the status of surface vegetation cover. It greatly supplements the environmental data required for studying invasive species, providing essential support for efficient and non-destructive pest monitoring (Gogoi et al., 2018). Kumbula et al. (2019) utilized remote sensing data from the Sentinel-2 MSI sensor to examine the potential distribution of the wood borer pest, *Coryphodema tristis* (Lepidoptera: Cossidae). Their findings indicated that utilizing remote sensing data and vegetation indices could yield highly accurate prediction outcomes. Therefore, large-scale vegetation index products obtained from remote sensing data can act as important environmental data for SDMs modeling. Using vegetation indices such as the Normalized Difference Vegetation Index (NDVI) and the Enhanced Vegetation Index (EVI), which are closely related to the "visible-near infrared" bands, often results in better model performance (Makori et al., 2017).

Currently, monitoring the temporal changes in pest suitability distribution mainly uses years or even decades as the basic unit. Through interannual analysis, it is possible to assess the efficacy of pest management strategies taken over the preceding period and to understand the species' responsiveness to environmental changes (Arenas-Castro and Sillero, 2021). The latter uses various climate models to predict the spatial distribution changes of pests under future climate change scenarios, allowing for combating outbreaks well in advance (Eigenbrode et al., 2017). For FAW, scholars have conducted numerous studies monitoring the changes in suitability distribution over decades (Ramasamy et al., 2022; Timilsena et al., 2022). These studies can predict changes in species distribution caused by climate change, providing valuable references for FAW risk assessment and integrated management. However, they often overlook the information hidden in seasonal variations. Due to the lack of diapause traits, FAW can only overwinter in tropical and subtropical regions. To reinvade planting areas in mid-latitude regions, it must initiate a series of new migrations each spring. We need to conduct time series analysis with higher temporal resolution to obtain this information, providing recommendations for more precise FAW control.

In addition to the environmental variables and time resolution, the SDMs also significantly impact the accuracy of pest monitoring. SDMs mainly include the correlative species distribution models and mechanistic species distribution models. Mechanistic models simulate the processes behind observed correlations with environmental factors (Beerling et al., 1995) by utilizing detailed knowledge of the target species' physiological responses to environmental factors and life-history traits (Stephenson, 1998). The parameterization of mechanistic models necessitates specialized scientific knowledge and crucial resources, which are currently inaccessible for numerous species, thus restricting their application (Shabani et al., 2015). Correlative models can be rapidly parameterized with minimal requirements, utilizing readily accessible distribution records and spatial environmental data. Examples of correlative models include Maximum Entropy (MaxEnt), Random Forest (RF), and Support Vector Machine (SVM). Among these, MaxEnt is particularly favored for exploring the potential distribution of FAW (Fan et al., 2021; Huang et al., 2020) due to its flexibility and performance.

Overall, research on pest suitability distribution is evolving towards multi-factor coupling analysis and refined temporal analysis. This study hopes to comprehensively consider both natural geographical conditions and vegetation cover status. By using annual distribution points and the MaxEnt model, it aims to establish an annual model to extract the global suitability distribution of FAW throughout the year. Furthermore, by combining seasonal distribution points and monthly environmental data, this study will establish monthly models for dynamic temporal monitoring, analyzing the distribution and changes of suitability distribution between different months. The research results can provide recommendations for timely and precise implementation of scientifically effective joint control measures, thereby preventing FAW from causing incalculable damage to crops in invaded areas.

2. Materials and Methods

2.1. Workflow for annual and monthly model

To commence, we categorized the historical occurrence records of FAW into annual and seasonal distribution points. By integrating multi-factor environmental data—comprising vegetation, meteorology, soil, and topography—we constructed a comprehensive environmental factor dataset. Subsequently, we optimized the MaxEnt model by selecting the most suitable parameter combinations, and applied the optimized MaxEnt model to establish both annual and monthly habitat suitability models. The annual model delineated the global distribution of suitable habitats for FAW across the year. For the annual model, we conducted an importance analysis of environmental variables, which included contribution rate assessments and a jackknife test(Warren and Seifert, 2011). For the monthly models, we extracted the distribution of suitable habitats for each of the 12 months. We then analyzed the contributions of dynamic environmental variables to the monthly models and examined the variations in habitat suitability between months (Fig. 1).

2.2. Multi-source data and preprocessing

2.2.1. Historical occurrence records of FAW and preprocessing

Historical occurrence records of FAW were mainly obtained from the Global Biodiversity Information Facility (GBIF, https://www.gbif.org/) (GBIF, 2023), domestic reports, and published international literature (Early et al., 2018; Goergen et al., 2016; Liao et al., 2019). These records cover the period from 1736 to 2023. After removing duplicates, a total of 2,984 records of FAW distribution were obtained. Using SDMtoolbox2.0 (https://www.sdmtoolbox.org)(Brown et al., 2017), the distribution data were processed by retaining only one record point per grid (10 km $\times$ 10 km) to avoid model overfitting caused by spatial autocorrelation, resulting in a final set of 1,309 FAW distribution points. Insects only begin to develop when the environmental temperature exceeds their developmental threshold temperature. The developmental threshold temperature determines whether an insect can complete its life cycle in a given area (Xiongkui et al., 2017). For FAW, the threshold temperature for the full generation development is typically around 10 °C (Ramirez Garcia et al., 1987). Therefore, distribution points where the minimum temperature of the coldest month exceeds 10 °C were classified as annual distribution points, whereas those below 10 °C were classified as seasonal distribution points (Fig. 2).

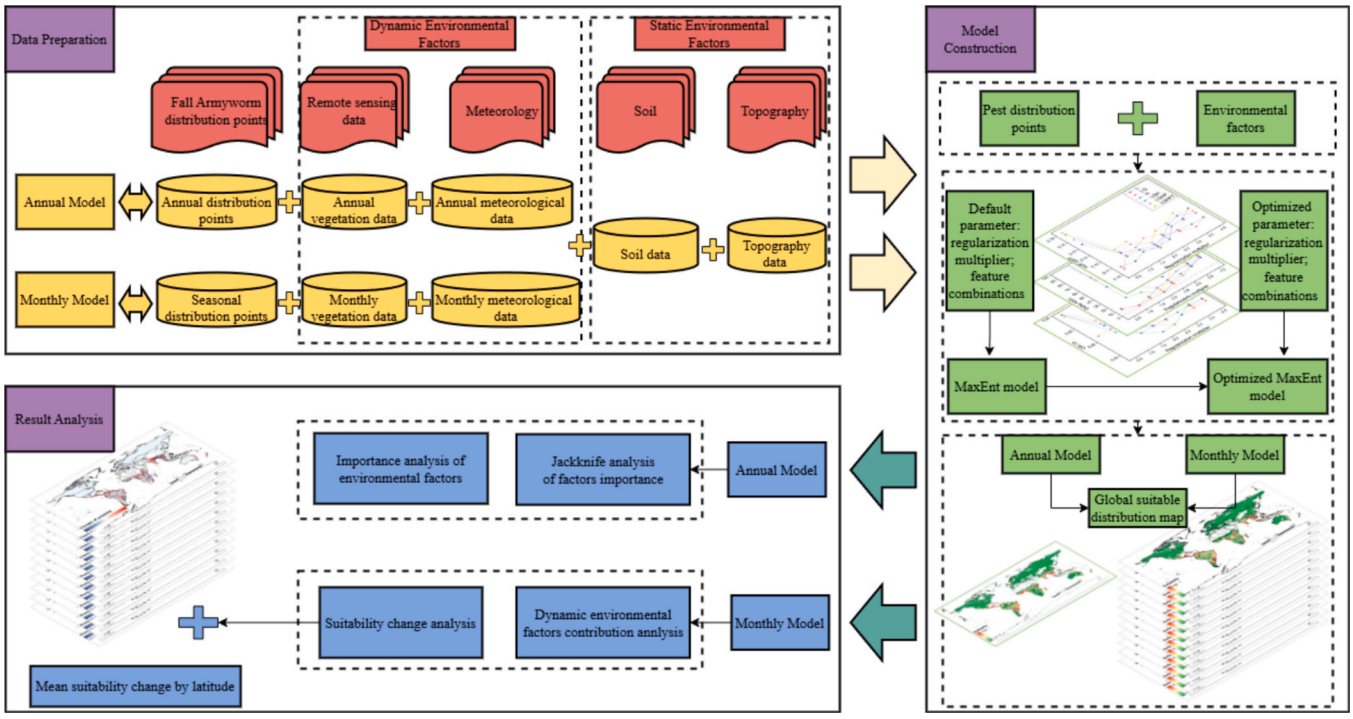


Fig. 1. Flowchart of the investigation.

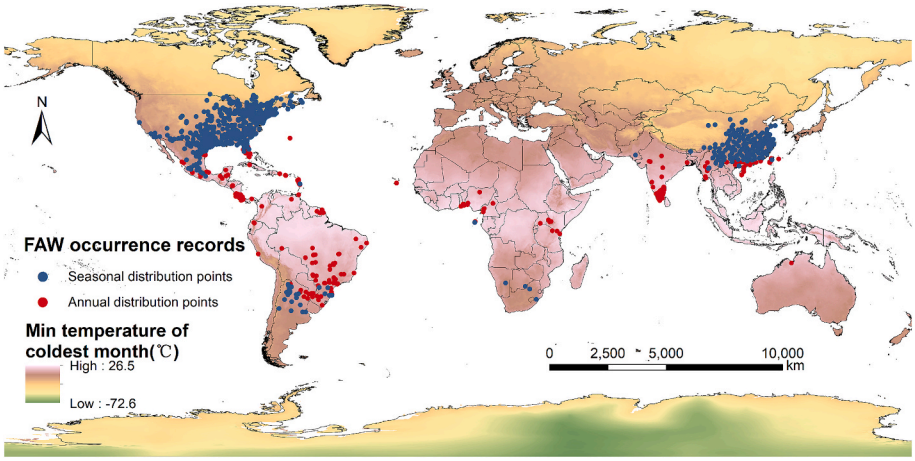


Fig. 2. Distribution of historical occurrence records of FAW worldwide (1736–2023).

2.2.2. Acquisition and preprocessing of meteorological data

The meteorological data used in this study were obtained from the WorldClim global climate database version 2.1 (https://worldclim.org) (Fick and Hijmans, 2017). We utilized historical climate data and historical monthly weather data for constructing the annual and monthly models, respectively.

The historical climate data include 19 bioclimatic variables (**Table S1**). In this study, we downloaded climate data with a resolution of 30″. Due to the correlations among the 19 bioclimatic variables (Yoon et al., 2021), we conducted a correlation analysis using SPSS software (Fig. 3). The historical occurrence records of FAW were incorporated with these bioclimatic variables to preliminarily build a MaxEnt model and determine the contribution rates of each variable. For variable groups with Pearson correlation values ≥ 0.8, we selected the variable with the highest contribution rate and excluded those with contribution rates below 5 %. Four bioclimatic variables were ultimately chosen for subsequent model building. These include two temperature variables: temperature seasonality (bio4) and max temperature of the warmest month (bio5), as well as two precipitation variables: annual precipitation (bio12) and precipitation of the driest quarter (bio17). Additionally, the historical monthly weather data include three available variables: precipitation (PREC), minimum temperature (TMIN), and maximum temperature (TMAX). In this study, we downloaded monthly data from 2000 to 2018 with a resolution of 2.5′ (approximately 4600 m). To standardize the resolution, we performed interpolation on the historical monthly weather data using the inverse distance weighting method to increase the resolution to 1000 m. The data from 2000 to 2018 were averaged to obtain monthly average data for each month of the year.

2.2.3. Acquisition and preprocessing of remote sensing data

The MODIS MOD13A2 product provides two vegetation indices: NDVI and EVI, with a temporal and spatial resolution of 16 days and 1 km, respectively. We downloaded the level-3 data for the period 2001–2021 from Google Earth Engine (https://earthengine.google.co

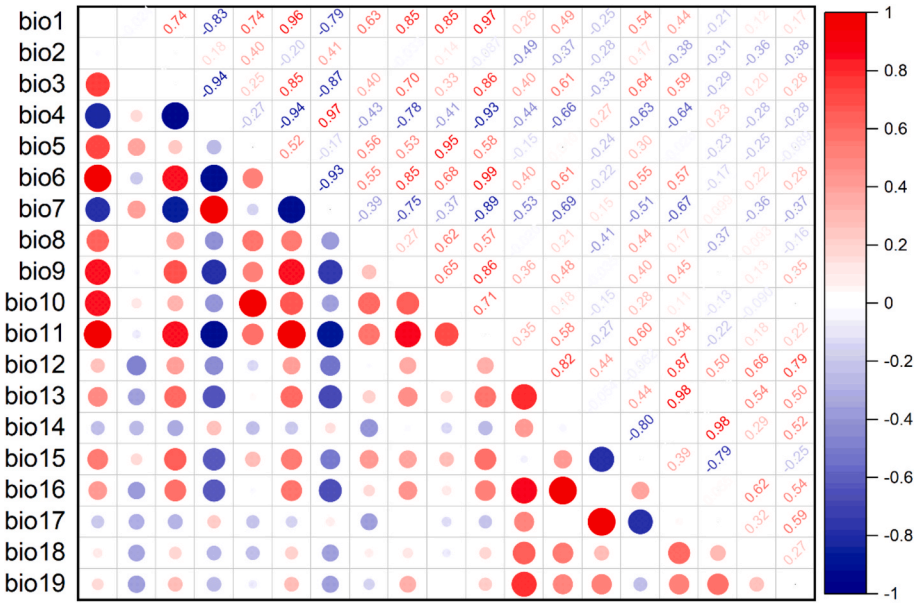


Fig. 3. Correlation matrix (Pearson) heatmap of meteorological environmental factors (1970–2000).

m/). For the purpose of constructing annual and monthly models, the vegetation index data underwent processing for "annual average" and "monthly average". The data used for the "annual mean" processing were filtered from January 1, 2001, to January 1, 2022, and then averaged over the 21-year period. For the "monthly mean" processing, the data were filtered from the first day of each month to the first day of the following month within the years 2001–2021, and then averaged within each month.

2.2.4. Acquisition of other data

The soil data were obtained from the Harmonized World Soil Database (HWSD), which provides grid data with a spatial resolution of 30 arc-seconds. This database includes information on soil types, soil phases, and soil physicochemical properties for each grid point. The soil data used in this study, updated in 2013, were retrieved from https://www.fao.org/soils-portal/data-hub/soil-maps-and-databases/harmonized-world-soil-database-v12/en/(Nachtergaele et al., 2009). In this study, we selected the Topsoil Clay Fraction (T_CLAY) and Topsoil Silt Fraction (T_SILT). Elevation data were obtained from the GTOPO30 dataset (Earth Resources Observation and Science Center, 1997), which was completed in 1996 with a resolution of 30 arc-seconds.

2.3. Model

2.3.1. Annual model

In this study, we first established an annual model based on MaxEnt. It simulates the potential geographic distribution of species within the natural environment using two input layers: historical occurrence records of the species and environmental factors. For the annual model, the input layer of species historical occurrence records only includes annual distribution points. The environmental variables utilized in this study can be divided into static and dynamic environmental factors (Table 1). The difference lies in that dynamic environmental factors vary more significantly with months compared to static environmental factors. The environmental data input layer (Layer-I) for the annual model includes meteorological data, vegetation index data, soil data, and topographic data. The first two categories are dynamic environmental factors, while the latter two belong to static environmental factors.

The significance of environmental factors influencing the potential geographic distribution of the species was assessed in the annual model using contribution rates and the jackknife test. At each step of the algorithm, the gain of the model is improved by adjusting the coefficients corresponding to each feature value, and the increased gain is attributed to the environmental factors that each feature value relies upon. At the end of the training process, the contribution is converted into a percentage, yielding the contribution rate for each environmental variable. Additionally, the MaxEnt model uses the jackknife test to evaluate the relative significance of environmental factors in predicting potential suitability distribution. The jackknife test involves omitting one environmental factor at a time and extracting the distribution area of FAW based on the remaining factors for the same study region, ultimately providing the importance of each environmental factor. In addition, the prediction results of this study were output in the "Logistic" format, and the final results were calculated as the average of 10 repetitions. Other parameters were kept at their default settings.

Table 1
The static and dynamic environmental factors extracted for the analyses of the suitability distribution of FAW.

Data Type	Environmental Factors	Abbreviation	Units
	Dynamic Environmental Factors		
Meteorological Data	Temperature Seasonality	bio4	1
	Max Temperature of Warmest Month	bio5	℃
	Annual Precipitation	bio12	mm
	Precipitation of Driest Quarter	bio17	mm
	Precipitation	PREC	℃
	Minimum Temperature	TMAX	℃
	Maximum Temperature	TMIN	mm
Vegetation Index Data	Normalized Difference Vegetation Index	NDVI	1
	Enhanced Vegetation Index	EVI	1
	Static Environmental Factors		
Soil Data	Topsoil Clay Fraction	T_CLAY	%wt
	Topsoil Silt Fraction	T_SILT	%wt
Topographic Data	Digital Elevation Model	DEM	m

2.3.2. Monthly model

We also established monthly models based on MaxEnt using annual distribution points and seasonal distribution points. The species historical occurrence record input layer of the monthly model combines annual distribution points with seasonal distribution points for each month. Compared to the annual model, the environmental factors in the

monthly model only varied in terms of dynamic environmental factors. Specifically, the meteorological data changed from bio4, bio5, bio12, and bio17 to PREC, TMAX, and TMIN. The environmental factors included in the vegetation index data remain unchanged, but their temporal resolution has been changed to a monthly basis, thus forming a new environmental data layer (Layer-II) as the input for the monthly model.

2.3.3. Model evaluation

Under default parameter settings, the MaxEnt model often does not represent the optimal model. Regularization multiplier (RM)and the feature combinations (FC) both significantly impact MaxEnt's predictive accuracy and complexity(Shcheglovitova and Anderson, 2013). To achieve optimal predictive performance and avoid model overfitting, the MaxEnt model was refined by adjusting the RM and FC(Morales et al., 2017). In this study, the RM ranged from 0.5 to 4.0, increasing by 0.5 increments. For FC, the MaxEnt model includes five feature types: linear (L), quadratic (Q), hinge (H), product (P), and threshold (T). Six feature combinations were selected for testing, namely L, LQ, H, LQH, LQHP, and LQHPT.

In this study, the model fit and complexity were evaluated using the corrected Akaike Information Criterion (AICc) (Akaike, 1974). Model overfitting was assessed by examining the difference between training and testing AUC (AUC.DIFF) and the 10 % training omission rate (OR.10) (Pearson et al., 2007). The AICc value represents the balance between model complexity and data fit. A lower AICc value indicates a higher degree of fit and better model performance (Warren and Seifert, 2011). Delta AICc is calculated by subtracting the smallest AICc value from the AICc value of each individual model. The parameter set yielding the lowest Delta AICc value was selected as the optimal configuration for model building. This study used the omission rate (OR) to assess the predictive ability of the model, reflecting how well it created with training data predicts the test data. OR.10 is a threshold-dependent measure that shows the percentage of test points with suitability values below the threshold, which excludes the 10 % of training points with the lowest predicted suitability. Higher omission rates exceeding the anticipated 10 % threshold typically indicate model overfitting.

3. Results

3.1. Anuual model

3.1.1. Optimal parameter combination for the annual model

The 48 parameter combinations of the annual model were evaluated using the assessment criteria within the ENMeval package. In Fig. 4, it could be seen that when RM = 2, FC = LQH, the model's AICc value was the smallest, indicating the lowest complexity. AUC.DIFF and OR.10 values were reduced by 15.6 % and 32.3 %, respectively, compared to the default parameters, suggesting minimal overfitting under these parameters. Thus, RM = 2 and FC = LQH were chosen as the optimal model parameters.

3.1.2. The suitability distribution map of the annual model and the importance analysis of environmental variables

The results of the MaxEnt model, run with the optimal parameter combination, were imported into ArcGIS 10.8 to obtain the global suitability distribution map for FAW (Fig. 5**A**). Additionally, based on land use data (MODIS land cover data, MCD12Q1), areas unsuitable for FAW survival were excluded. These areas include impervious surfaces, wetlands, snow-covered regions, deserts, and water bodies. The prediction results indicate that areas with high suitability for FAW in the Americas are distributed in the southern coastal regions of the United States, Central America, Venezuela, Colombia, Brazil, Argentina, and Paraguay. In Europe, the distribution is relatively smaller compared to other continents, mainly concentrated in the Iberian Peninsula and surrounding the Mediterranean region. In Africa, the main distribution is in equatorial countries such as Cameroon, Benin, Ghana, Liberia, Sierra Leone, Ivory Coast, Sudan, Ethiopia, and Uganda. In Asia, the primary distribution is in the Indian Peninsula, Indochina Peninsula, the Philippines, and southern China. In Oceania, the main distribution is along the coastal areas of Australia and New Guinea Island. Most of these regions are located near the equator, and these areas experience tropical and subtropical climates that offer enough heat for FAW growth and breeding even during the coldest months.

The contribution rates of the environmental variables in Layer-I are shown in Fig. 5**B**. It can be seen that bio4 (Temperature Seasonality) is the primary limiting factor for the suitability of FAW, with a single-factor contribution rate of 39.87 %. T_SILT (Topsoil Silt Fraction) has the least impact on the distribution of the annual suitability of FAW, with a single-factor contribution rate of 3.42 %. Fig. 5**C** presents the results of the jackknife test, evaluating the relative importance of environmental variables in predicting potential suitability distribution. Bio4 achieves the highest gain when used in isolation among the environmental variables, indicating that it provides the most useful information on its own. It is followed by bio12, EVI, NDVI, bio5, and T_CLAY, all of which have gains greater than 0.6 when used in isolation. The omission of bio4 results in the greatest reduction in gain, suggesting that it provides the most unique information not captured by the other variables.

3.2. Monthly model

3.2.1. The suitability distribution map of the monthly model

The models for January to December were constructed by incorporating seasonal distribution points and Layer-II variables. **Table S2**

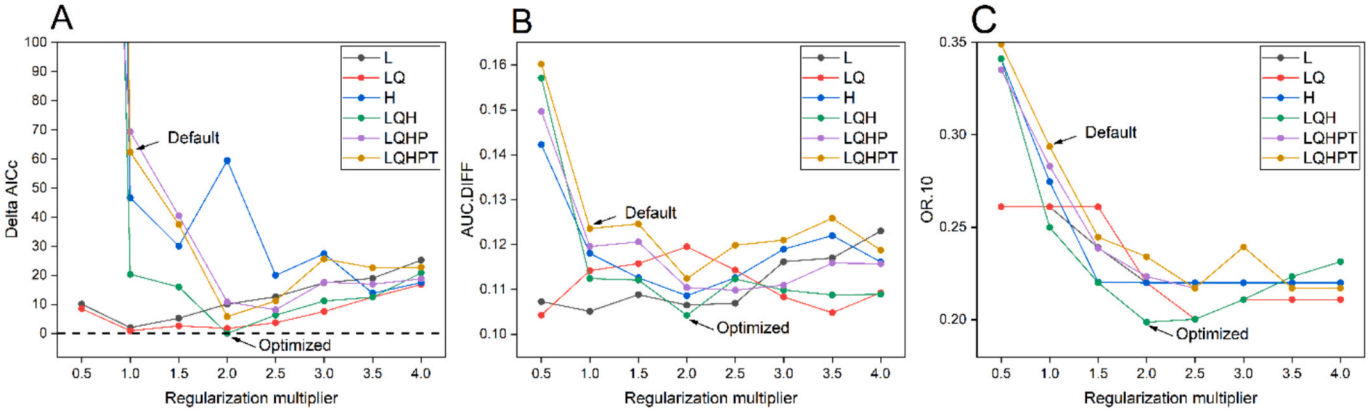


Fig. 4. AUC.DIFF and OR10 for FAW resulting from Maxent models under different parameter combinations.

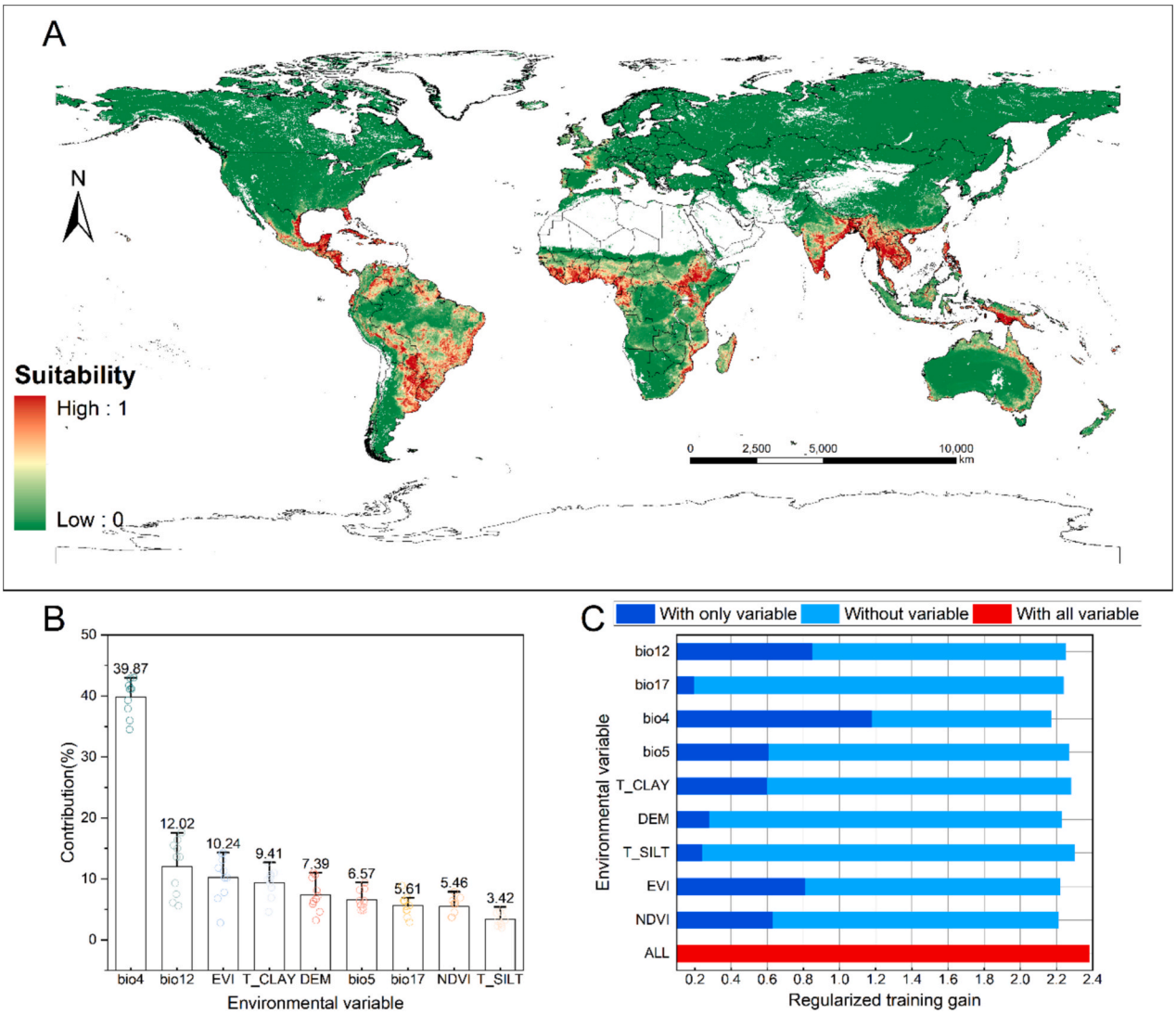


Fig. 5. Global suitability distribution map of the annual models and environmental variable analysis. (A) Annual suitability distribution map of FAW globally; (B) Average contribution of each environmental variable in Layer-I; (C) Jackknife analysis of variable importance.

shows the results after parameter optimization using ENMeval. Using the optimal parameter combinations, monthly models were established to obtain suitability distribution maps for FAW from January to December on a global scale (Fig. 6). Similarly, regions unsuitable for FAW survival were excluded. To further understand the monthly distribution of FAW suitability, we plotted the latitude distribution lines of mean suitability for FAW from January to December (Fig. 7). The figure shows that FAW's suitability distribution are primarily located in tropical regions, expanding into temperate regions as the months progress. Table 2 presents the three parameters extracted from the latitude distribution lines of mean suitability shown in Fig. 7. The magnitude of the mean suitability area under the curve (S_AUC) value is determined by the suitability values and the range of suitable areas within that month. Therefore, it represents the mean suitability of FAW in that month to some extent. Calculations show that among the months from January to December, the S_AUC value is highest in July and lowest in March. Additionally, we obtained the boundary latitudes of the distribution line, defined as the boundaries where the mean suitability is greater than 0.01. It can be seen that from August to December, the boundaries of suitable areas in both the northern and southern hemispheres gradually shift southward, while the trend is reversed from January to July. Similar to the changes in S_AUC values, the months with the largest and smallest ranges of boundary latitudes are also July and March, respectively.

3.2.2. *Analysis of the contribution rates of environmental variables in monthly model*

In this study, the dynamic environmental factors used in the monthly model were categorized into three types: temperature (TEM), precipitation (PRE), and vegetation index (VI). These three factors are also key indicators reflecting seasonal changes. Fig. 8 shows the contribution rates of seasonal indices composed of dynamic environmental factors. It can be observed that with the change of months, the contribution rate of TEM first increases and then decreases, while the contribution rate of VI shows the opposite trend. The contribution rate of PRE, except for a peak in September, remains relatively stable despite some fluctuations in other months. It is also worth noting that the overall contribution rate of the three seasonal indicators from January to December reached about 80 %. This highlights the dominant role that dynamic environmental factors, including vegetation indices, play in the monthly variation of FAW suitability distribution.

3.2.3. *Monthly model suitability change analysis*

Furthermore, this study compared the suitability distribution for FAW from January to December in pairs, resulting in 12 global spatial variation maps of FAW suitability distribution (**Fig. S1**). To more

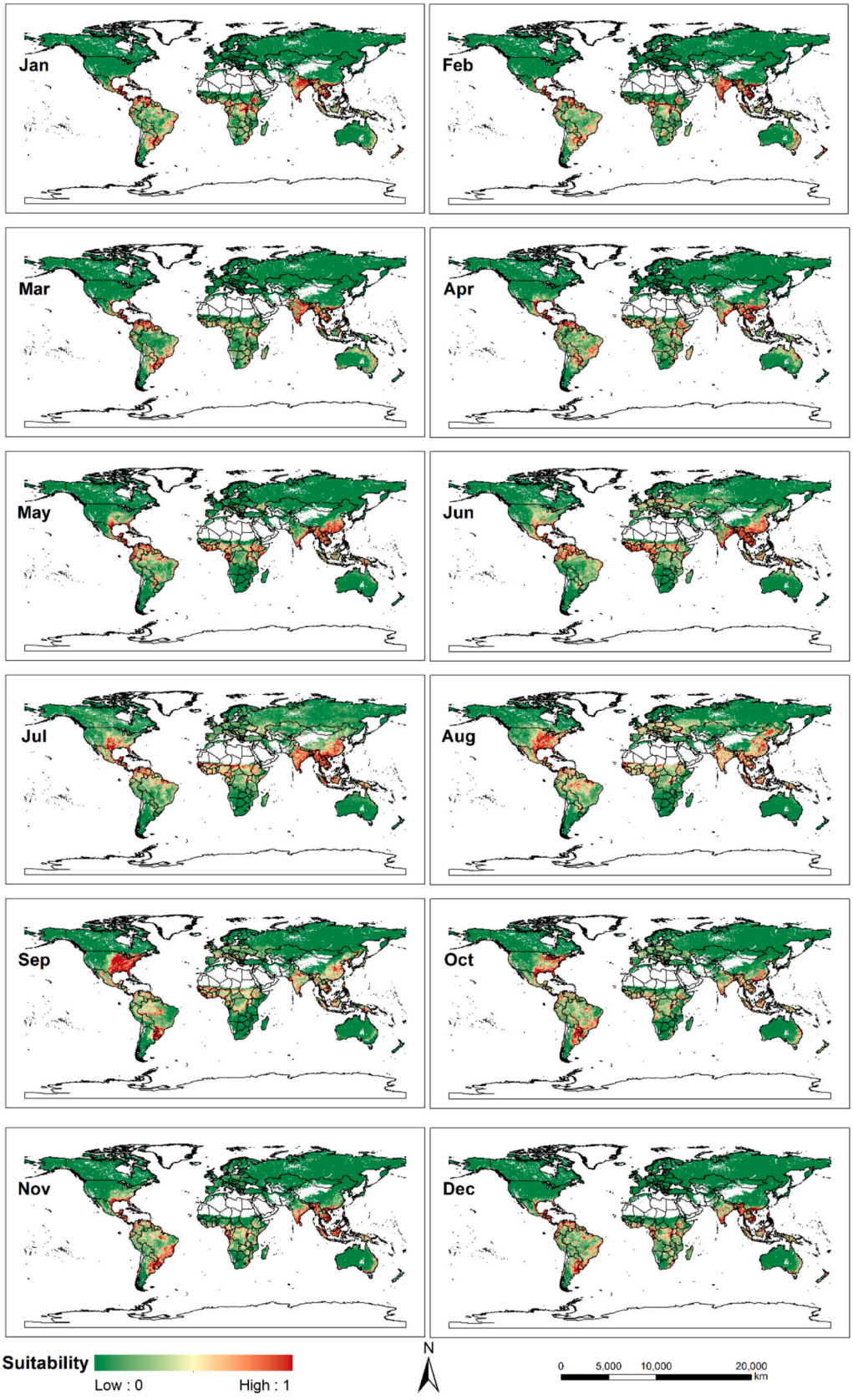


Fig. 6. Suitability distribution of FAW from January to December.

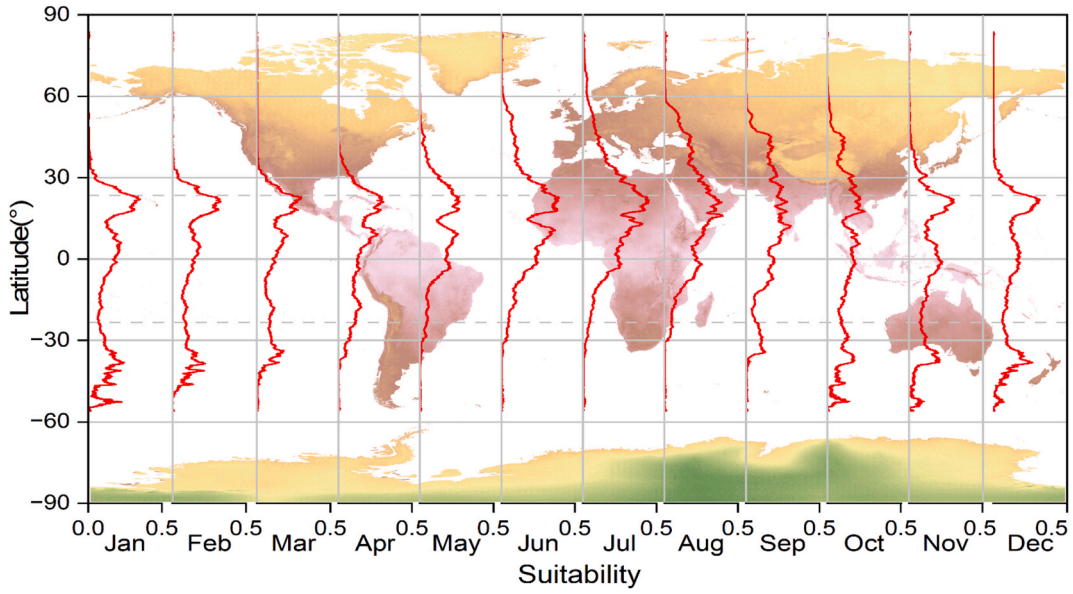


Fig. 7. Latitudinal and monthly variations in the mean suitability of FAW. The horizontal axis represents the mean suitability values for each month. The red curve illustrates the monthly variations in mean suitability across latitudes, while the dashed lines indicate the Tropic of Cancer and the Tropic of Capricorn. (For interpretation of the references to colour in this figure legend, the reader is referred to the web version of this article.)

Table 2
Parameters of the mean suitability latitude distribution line.

Month	S_AUC	Northern Latitude	Southern Latitude
1	12.37426	41.22268°N	55.95469°S
2	10.67791	37.76425°N	55.93672°S
3	9.30466	36.78511°N	46.30702°S
4	10.28338	39.09372°N	40.04591°S
5	9.58193	48.64258°N	34.78191°S
6	14.40543	60.88632°N	34.85378°S
7	16.71796	77.08254°N	35.98563°S
8	15.93369	58.55974°N	30.30841°S
9	13.80796	55.12826°N	39.81236°S
10	13.19561	58.60465°N	54.49945°S
11	11.66623	46.44176°N	55.93672°S
12	10.59439	39.09372°N	55.95469°S

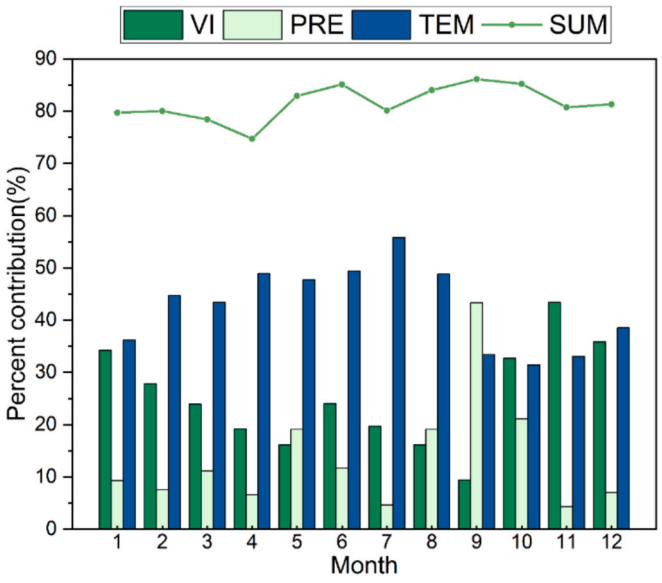


Fig. 8. Contribution rates of seasonal variables in monthly models. SUM represents the combined contribution rates of the three types of dynamic variables.

intuitively understand the latitudinal changes in FAW suitability between months, we calculated the mean suitability change for each latitude (Fig. 9). From the figure, it can be seen that the mean suitability change in the Northern Hemisphere is mostly greater than zero from March to April, April to May, May to June, and June to July. This indicates that the suitability for FAW in the Northern Hemisphere is generally in an increasing state from March to July. Additionally, it can be noted that the latitudes with positive change values gradually extend northward, indicating that the FAW suitability distribution is shifting northward over time. From July to August, the change values in some latitudes of the Northern Hemisphere turns negative, indicating a decrease in suitability distribution. From August to September, September to October, and October to November, the latitudes with negative change values further increase, showing a significant reduction in FAW suitability distribution in the Northern Hemisphere. However, from November until March of the following year, fluctuation is relatively small. In contrast, the Southern Hemisphere experiences the opposite trend: from January to May, most change values are negative, indicating a gradual reduction in suitability distribution; from May to August, fluctuation is relatively small; from August to January of the following year, change values turn positive, with suitability distribution gradually increasing.

4. Discussion

In this study, the environmental variables used for constructing the models were divided into static and dynamic categories. While it may be contended that no variable is entirely static(Stanton et al., 2012), for practical purposes, we defined variables that change very slowly as “static” variables, whose cumulative changes over the modeling period can be considered negligible (e.g., soil conditions). In contrast, variables that undergo significant changes over time were defined as “dynamic” variables (e.g., meteorology variables). In the annual model, the contribution rates of static and dynamic environmental variables were 20.2 % and 79.8 %, respectively. In the monthly model, the contribution rates of dynamic environmental variables composed of PRE, TEM, and VI were also around 80 %. The trend of suitability changes in the monthly model aligns closely with the seasonal alternation of the Northern and Southern Hemispheres, indicating that dynamic environmental variables such as temperature and precipitation are the primary

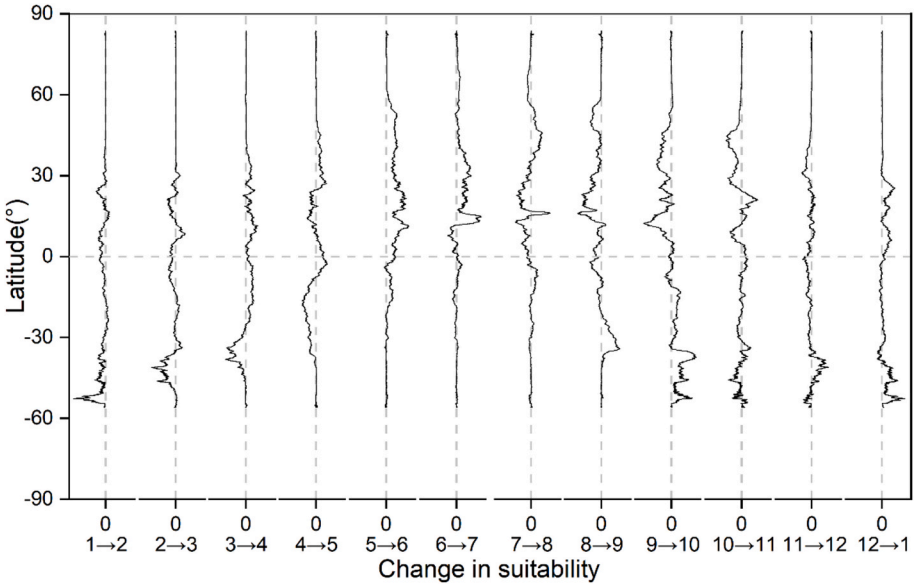


Fig. 9. Latitudinal variations in monthly changes of FAW suitability. The horizontal axis represents the changes in mean suitability values between months.

drivers of changes in FAW suitability distribution. Two types of environmental variables are indispensable in the model construction. Static environmental variables provide a stable background, mainly influencing the model through their impact on the basic structure and characteristics of the environment. Dynamic environmental variables reflect the spatial and temporal variations in the environment, capturing seasonal variations and climate fluctuations. Consequently, the final model results from the synergistic impact of these two categories of environmental variables.

Remote sensing data facilitates instantaneous monitoring and near-term forecasting of FAW distribution (Huang et al., 2020). This study utilized the vegetation index products from MODIS as part of the environmental data input. In the annual model, the total contribution rate of vegetation environmental factors reached 15 %. Although the contribution of vegetation data varied in different months in the monthly model, the minimum contribution was 9.4 %, and the maximum reached 35.8 %. This demonstrates the importance of vegetation data factors in extracting suitability distribution for FAW. It also highlights the broad application potential of remote sensing data and products in predicting species suitability distribution. Currently, remote sensing is extensively utilized for monitoring and predicting plant diseases and pests (Zhang et al., 2019). We also anticipate that remote sensing will play an even more significant and effective role in the future efforts to prevent and control FAW.

Previous studies often did not distinguish between the historical occurrence records of FAW. Seasonal distribution points are not suitable for extracting annual suitability distribution, as they assume that the locations of historical occurrence records always represent suitability distribution. This assumption can lead to misjudgments in the final model (El-Gabbas et al., 2021). In this study, we differentiated the historical occurrence records into annual distribution points and seasonal distribution points based on the minimum temperature of the coldest month at each location. Using this classification, we established separate annual and monthly models to capture both the perennial and temporal dynamics of FAW distribution. The annual model highlights long-term high-risk areas globally, identifying regions that require consistent monitoring and control measures. These measures may include the establishment of FAW control demonstration zones, the enhancement of plant protection infrastructure, and the introduction of natural enemies to mitigate the pest's impact. In contrast, the monthly model provides detailed insights into the seasonal dynamics of FAW's suitable habitats, offering practical guidance for spatiotemporally targeted management strategies. For instance, during periods of habitat expansion, preventive measures such as insecticide spraying or trapping techniques can be deployed proactively. Conversely, during periods of contraction, pesticide usage can be reduced, minimizing both environmental impact and economic costs. Moreover, the monthly model reveals broader spatial patterns of suitability fluctuations in response to seasonal environmental changes. Through the analyses of the results from the monthly model, we observed that as time approaches the summer months, the fluctuation becomes more significant, while as it approaches the winter months, the fluctuation diminishes. This may be because the favorable summer conditions for FAW allow the already suitable regions to become even more conducive to FAW survival, leading to an expansion of their suitability distribution. In contrast, the winter conditions restrict FAW to certain areas, which are often the regions with higher suitability values in the annual model.

The occurrence of FAW is a multi-stage process influenced by various factors such as bioclimate, soil conditions, and host vegetation. This complexity is especially pronounced when studying on a global scale, where the differences and complexities of environmental factors become more evident. Therefore, when establishing models, the input of environmental factors has always been a key determinant of the model's predictive accuracy. Maino et al. (2021) emphasized that incorporating the associated FAW mortality and natural enemies will be crucial in future models aimed at enhancing the predictability of outbreaks. Additionally, in future research, using different environmental factors as inputs for different regions might be a way to improve model accuracy. Furthermore, this study only considers the potential global suitability distribution for FAW under the current climatic conditions based on historical occurrence records and environmental factors. Significant impacts of dynamic environmental variables, such as temperature, precipitation, and vegetation, on FAW suitability have been observed. Therefore, the potential influence of climate change on FAW's suitability distribution should be considered in future research.

5. Conclusions

This study combined traditional environmental data with remote sensing data to establish an environmental factor dataset that includes meteorology, vegetation, soil, and topography. Based on this dataset, annual and monthly models were developed using MaxEnt. To select the best MaxEnt model, the study used the ENMeval package to evaluate model performance through metrics such as AICc, AUC.DIFF, and

OR.10, optimizing the parameter combinations of the MaxEnt model. The optimization results for the annual model indicated that when FC = LQH and RM = 2, the annual model had the smallest AICc. At this point, the AUC.DIFF and OR.10 values were reduced by 15.6 % and 32.3 %, respectively, compared to the default parameters.

We used annual distribution points from the FAW distribution data as input for the annual model data layer, resulting in the annual suitability distribution of FAW worldwide. The results indicate that FAW mainly distributes in central South America, southern North America, central Africa, and regions near the equator in South Asia and Southeast Asia. Among all the environmental variables used, bio4 (Temperature Seasonality) had the greatest impact on the FAW's suitability distribution, with a single-variable contribution rate of 39.87 %. Additionally, the combined contribution rate of vegetation index data reached 15 %, confirming the importance of vegetation index factors in extracting FAW's suitability distribution and demonstrating the effective application of remote sensing data in this work. In the future, it can be integrated with ground-based surveys to assist governments and farmers in developing more targeted pest control strategies, ultimately contributing to the achievement of global food security goals.

By aligning the temporal resolution of dynamic environmental factors with FAW occurrence records on a monthly basis, we established monthly models to analyze the spatial variation of FAW suitability distribution from January to December. The analysis revealed that FAW suitability is highest in July and lowest in March. Additionally, the changes in suitability between months exhibit distinct seasonal variation patterns. Environmental variables such as TEM (temperature), PRE (precipitation), and VI (vegetation index) showed high contribution rates, with their total contribution exceeding 80 % for each month. This demonstrates that these seasonal indicators are the dominant factors driving the inter-monthly variation in suitability distribution. This also indicates that the monthly model established in this study can reveal the spatial variation in suitability distribution, responding to seasonal environmental changes. This research provides methodological support for precise early warning and effective control of FAW, helping to significantly reduce pesticide use and ensure global food security.

CRediT authorship contribution statement

Minghao Wang: Writing – original draft, Visualization, Validation, Software, Methodology, Formal analysis, Conceptualization. **Wenjiang Huang:** Writing – review & editing, Supervision, Funding acquisition. **Yingying Dong:** Writing – review & editing, Resources, Project administration, Investigation, Data curation. **Yanru Huang:** Resources, Methodology, Investigation, Data curation. **Bing Zhang:** Resources, Methodology, Investigation, Data curation. **Gang Sun:** Resources, Methodology, Investigation, Data curation. **Maged Elkahky:** Resources, Methodology, Investigation, Data curation. **Changping Huang:** Resources, Methodology, Investigation, Data curation.

Funding

This work was supported by National Natural Science Foundation of China (Grant No.42071320), funded by Fengyun Application Pioneering Project (Grant No. FY-APP-2022.0306), FAO Yanbao funding.

Declaration of competing interest

The authors declare that they have no known competing financial interests or personal relationships that could have appeared to influence the work reported in this paper.

Appendix A. Supplementary data

Supplementary data to this article can be found online at https://doi.org/10.1016/j.ecolind.2025.113181.

Data availability

Data will be made available on request.

References

Akaike, H., 1974. A new look at the statistical model identification. IEEE Transactions on Automatic Control 19 (6), 716–723.
Arenas-Castro, S., Sillero, N., 2021. Cross-scale monitoring of habitat suitability changes using satellite time series and ecological niche models. Science of the Total Environment 784, 147172.
Beerling, D.J., Huntley, B., Bailey, J.P., 1995. Climate and the distribution of Fallopia japonica: use of an introduced species to test the predictive capacity of response surfaces. Journal of Vegetation Science 6 (2), 269–282.
Brown, J.L., Bennett, J.R., French, C.M., 2017. SDMtoolbox 2.0: the next generation Python-based GIS toolkit for landscape genetic, biogeographic and species distribution model analyses. Peerj. 5, e4095.
De Freitas Bueno, R.C.O., De Freitas Bueno, A., Moscardi, F., Postali Parra, J.R., Hoffmann-Campo, C.B., 2011. Lepidopteran larva consumption of soybean foliage: basis for developing multiple-species economic thresholds for pest management decisions. Pest Management Science. 67, 170–174.
Early, R., Gonzalez-Moreno, P., Murphy, S.T., Day, R., 2018. Forecasting the global extent of invasion of the cereal pest Spodoptera frugiperda, the fall armyworm. Neobiota. 40, 25–50. https://doi.org/10.3897/neobiota.40.28165.
Earth Resources Observation and Science Center, U. S. G. S., U.S. Department of the Interior. 1997. USGS 30 ARC-second Global Elevation Data, GTOPO30 . C. a. I. S. L. Research Data Archive at the National Center for Atmospheric Research, Version 2.0. https://doi.org/10.5065/A1Z4-EE71.
Eigenbrode, S. D., Macfadyen, S., and Langridge, P. J. A. s. c. o. w., 2017. The impact of climate change on wheat insect pests: current knowledge and future trends. 1, 545-567.
El-Gabbas, A., Van Opzeeland, I., Burkhardt, E., Boebel, O., 2021. Dynamic species distribution models in the marine realm: predicting year-round habitat suitability of baleen whales in the southern ocean. Frontiers in Marine Science. 08. https://doi.org/10.3389/fmars.2021.802276.
Fan, J., Haseeb, M., Ren, Q., Tian, T., Zhang, R., Wu, P., 2021. Factoring distribution and prevalence of Fall armyworm in southwest China. Journal of Applied Entomology. 145 (4), 295–302.
Fick, S.E., Hijmans, R.J., 2017. WorldClim 2: new 1-km spatial resolution climate surfaces for global land areas. International Journal of Climatology. 37 (12), 4302–4315. https://doi.org/10.1002/joc.5086.
GBIF. 2023. GBIF Occurrence Download. https://www.gbif.org/ (accessed 17 April 2023).
Giri, C.P., 2016. Remote sensing of land use and land cover: principles and applications. CRC Press.
Goergen, G., Kumar, P.L., Sankung, S.B., Togola, A., Tamo, M., 2016. First Report of Outbreaks of the Fall Armyworm Spodoptera frugiperda (J E Smith) (Lepidoptera, Noctuidae), a New Alien Invasive Pest in West and Central Africa. Plos One 11 (10), 9. https://doi.org/10.1371/journal.pone.0165632.
Gogoi, N., Deka, B., Bora, L., 2018. Remote sensing and its use in detection and monitoring plant diseases: A review. Agricultural Reviews. 39 (4).
Hardke, J.T., Lorenz, G.M., Leonard, B.R., 2015. Fall armyworm (Lepidoptera: Noctuidae) ecology insouth-eastern cotton. Journal of Integrated Pest Management. 6, 10.
Huang, Y.R., Dong, Y.Y., Huang, W.J., Ren, B.Y., Deng, Q.Y., Shi, Y., Ma, H.Q., 2020. Overwintering distribution of fall armyworm (Spodoptera frugiperda) in Yunnan, China, and influencing environmental factors. Insects 11 (11), 14. https://doi.org/10.3390/insects11110805.
Kenis, M., Benelli, G., Biondi, A., Calatayud, P.-A., Day, R., Desneux, N., Wu, K., 2023. Invasiveness, biology, ecology, and management of the fall armyworm, Spodoptera Frugiperda. Entomologia Generalis 43 (2), 187–241. https://doi.org/10.1127/entomologia/2022/1659.
Kumar, S., Graham, J., West, A.M., Evangelista, P.H., 2014. Using district-level occurrences in MaxEnt for predicting the invasion potential of an exotic insect pest in India. Computers Electronics in Agriculture 103, 55–62.
Kumbula, S.T., Mafongoya, P., Peerbhay, K.Y., Lottering, R.T., Ismail, R., 2019. Using sentinel-2 multispectral images to map the occurrence of the cossid moth (Coryphodema tristis) in eucalyptus nitens plantations of Mpumalanga, South Africa. Remote Sensing 11 (3), 16. https://doi.org/10.3390/rs11030278.
Liao, Y.L., Yang, B., Xu, M.F., Lin, W., Wang, D.S., Chen, K.W., Chen, H.Y., 2019. First report of Telenomus remus parasitizing Spodoptera frugiperda and its field parasitism in southern China. Journal of Hymenoptera Research 73, 95–102. https://doi.org/10.3897/jhr.73.39136.
Liu, T., Wang, J., Hu, X., Feng, J., 2020. Land-use change drives present and future distributions of Fall armyworm, Spodoptera frugiperda (JE Smith)(Lepidoptera: Noctuidae). Science of the Total Environment 706. https://doi.org/10.1016/j.scitotenv.2019.135872.
Maino, J.L., Schouten, R., Overton, K., Day, R., Ekesi, S., Bett, B., Reynolds, O.L., 2021. Regional and seasonal activity predictions for fall armyworm in Australia. Current Research in Insect Science. 1, 100010.
Makori, D.M., Fombong, A.T., Abdel-Rahman, E.M., Nkoba, K., Ongus, J., Irungu, J., Landmann, T., 2017. Predicting spatial distribution of key honeybee pests in Kenya using remotely sensed and bioclimatic variables: key honeybee pests distribution

models. Isprs International Journal of Geo-Information. 6 (3), 20. https://doi.org/10.3390/ijgi6030066.
Matova, P.M., Kamutando, C.N., Magorokosho, C., Kutywayo, D., Gutsa, F., Labuschagne, M., 2020. Fall-armyworm invasion, control practices and resistance breeding in Sub-Saharan Africa. Crop Science. 60 (6), 2951–2970. https://doi.org/10.1002/csc2.20317.
Montezano, D.G., Specht, A., Sosa-Gómez, D.R., Roque-Specht, V.F., Sousa-Silva, J.C., Paula-Moraes, S.V., Hunt, T.E., 2018. Host Plants of Spodoptera frugiperda (Lepidoptera: Noctuidae) in the Americas. African Entomology. 26 (2), 286–300.
Morales, N.S., Fernandez, I.C., Baca-Gonzalez, V., 2017. MaxEnt's parameter configuration and small samples: are we paying attention to recommendations: A systematic review. Peerj. 5, 16. https://doi.org/10.7717/peerj.3093.
Nachtergaele, F., Velthuizen, H., Verelst, L., Wiberg, D. J. F., and Agriculture Organization of the United Nations, R., 2009. Harmonized world soil database (hwsd).
Otim, M.H., Tay, W.T., Walsh, T.K., Kanyesigye, D., Adumo, S., Abongosi, J., Agona, A., 2018. Detection of sister-species in invasive populations of the fall armyworm Spodoptera frugiperda (Lepidoptera: Noctuidae) from Uganda. Plos One 13 (4), 18. https://doi.org/10.1371/journal.pone.0194571.
Pearson, R.G., Raxworthy, C.J., Nakamura, M., Townsend Peterson, A., 2007. Predicting species distributions from small numbers of occurrence records: a test case using cryptic geckos in Madagascar. Journal of Biogeography 34 (1), 102–117.
Pitre, H.N., Hogg, D.B., 1983. Development of the fall armyworm on cotton, soybean and corn. Journal of the Georgia Entomology Society 18 (2), 182–187.
Ramasamy, M., Das, B., Ramesh, R., 2022. Predicting climate change impacts on potential worldwide distribution of fall armyworm based on CMIP6 projections. Journal of Pest Science 95 (2), 841–854. https://doi.org/10.1007/s10340-021-01411-1.
Ramirez Garcia, L., Bravo Mojica, H., Llanderal Cazares, C., 1987. Development of Spodoptera frugiperda (JE Smith)(Lepidoptera: Noctuidae) under different conditions of temperature and humidity. Agrociencia 67, 161–171.
Shabani, F., Kumar, L., Taylor, S., 2015. Distribution of date palms in the middle east based on future climate scenarios. Experimental Agriculture 51 (2), 244–263.
Shcheglovitova, M., Anderson, R.P., 2013. Estimating optimal complexity for ecological niche models: A jackknife approach for species with small sample sizes. Ecological Modelling 269, 9–17. https://doi.org/10.1016/j.ecolmodel.2013.08.011.
Sisay, B., Simiyu, J., Mendesil, E., Likhayo, P., Ayalew, G., Mohamed, S., Tefera, T., 2019. Fall armyworm, Spodoptera frugiperda infestations in east africa: assessment of damage and parasitism. Insects 10 (7), 10. https://doi.org/10.3390/insects10070195.
Sparks, A.N., 1979. A review of the biology of the fall armyworm. Florida Entomologist 62 (2), 82–87.
Stanton, J.C., Pearson, R.G., Horning, N., Ersts, P., Akcakaya, H.R., 2012. Combining static and dynamic variables in species distribution models under climate change. Methods in Ecology and Evolution 3 (2), 349–357. https://doi.org/10.1111/j.2041-210X.2011.00157.x.
Stephenson, N., 1998. Actual evapotranspiration and deficit: biologically meaningful correlates of vegetation distribution across spatial scales. Journal of Biogeography 25 (5), 855–870.
Suby, S.B., Soujanya, P.L., Yadava, P., Patil, J., Subaharan, K., Prasad, G., Rakshit, S., 2020. Invasion of fall armyworm (Spodoptera frugiperda) in India: nature, distribution, management and potential impact. Current Science. 119 (1), 44–51. https://doi.org/10.18520/cs/v119/i1/44-51.
Timilsena, B.P., Niassy, S., Kimathi, E., Abdel-Rahman, E.M., Seidl-Adams, I., Wamalwa, M., Subramanian, S., 2022. Potential distribution of fall armyworm in Africa and beyond, considering climate change and irrigation patterns. Scientific Reports 12 (1). https://doi.org/10.1038/s41598-021-04369-3.
Warren, D.L., Seifert, S.N., 2011. Ecological niche modeling in Maxent: the importance of model complexity and the performance of model selection criteria. Ecological Applications 21 (2), 335–342. https://doi.org/10.1890/10-1171.1.
Westbrook, J.K., Nagoshi, R.N., Meagher, R.L., Fleischer, S.J., Jairam, S., 2016. Modeling seasonal migration of fall armyworm moths. International Journal of Biometeorology. 60 (2), 255–267. https://doi.org/10.1007/s00484-015-1022-x.
Xiongkui, H., Bonds, J., Herbst, A., Langenakens, J., 2017. Recent development of unmanned aerial vehicle for plant protection in East Asia. International Journal of Agricultural Biological Engineering. 10 (3), 18–30.
Yoon, S., Lee, W.-H. J. C., and Agriculture, E. i., 2021. Methodological analysis of bioclimatic variable selection in species distribution modeling with application to agricultural pests (Metcalfa pruinosa and Spodoptera litura). 190, 106430.
Zhang, J., Huang, Y., Pu, R., Gonzalez-Moreno, P., Yuan, L., Wu, K., Huang, W., 2019. Monitoring plant diseases and pests through remote sensing technology: A review. Computers and Electronics in Agriculture. 165. https://doi.org/10.1016/j.compag.2019.104943.